Supplementary information

Liquid Crystal-Like Active Layer for High-Performance Organic Field-Effect Transistors

Zhifang Wang†,[1,2,3] Daniel Martin-Jimenez†,[4] Yingying Zhang,[1] Miguel Wiche,[4] Lacheng Liu,[2] Daniel Ebeling,[4] Qigang Zhong,[4] Florian Fontein,[2] Andre Schirmeisen,[4] Lizhen Huang,[1] Zi Wang,*[5] Wenchong Wang,*[2,3] Lifeng Chi*[1,2,3]

1. Institute of Functional Nano & Soft Materials (FUNSOM), Jiangsu Key Laboratory for Carbon-Based Functional Materials & Devices, Soochow University, 199 Ren'ai Road, Suzhou, 215123, Jiangsu, P.R. China. E-mail: chilf@suda.edu.cn
2. Westfälische Wilhelms-Universität Münster, Physikalisches Institut and Center for Nanotechnology (CeNTech), Wilhelm-Klemm-Straße 10, 48149 Münster, Germany. E-mail: wangw@uni-muenster.de
3. Institution Center for Soft Nanoscience, Busso-Peus-Strasse10, 48149 Münster, Germany.
4. Institute of Applied Physics (IAP) and Center for Materials Research (LaMa), Justus Liebig University Gießen, Heinrich-Buff-Ring 16, 35392 Gießen, Germany.
5. Gusu Laboratory of Materials, 388 Ruoshui Road, Suzhou 215123, P.R. China. E-mail: wangzi2020@gusulab.ac.cn

Morphological characterization of semiconductor layer

The AFM images were analysed by WSxM softwire. The flooded AFM images in Fig. S2 were created by this software. When the thickness of dif-TES-ADT was 2 nm, the minimum height of the hills in Fig. S2a was set as exposed SiO_2 surface, that is, the blue area is the SiO_2 surface. Dif-TES-ADT islands occupy 26.17% of the surface area, and the average roughness of 2.47 nm can be read from the software. The PTCDI-C_{13} film in Fig. S2c was flooded to obtain the surface area of the dif-TES-ADT submonolayer (59.00%) by setting the minimum height to 3.2 nm, which is higher than the thickness of the PTCDI-C_{13} monolayer but not higher than the height of the dif-TES-ADT submonolayer grown on PTCDI-C_{13}. When the thickness of dif-TES-ADT was increased to 15 nm, we set the minimum heights to 1.3 nm and 3 nm on the SiO_2 surface and PTCDI-C_{13} surface, respectively, as shown in Fig. S2b and d, both resulting in dif-TES-ADT films occupying more than 99% of the surface area. The 15 nm dif-TES-ADT films grown on PTCDI-C_{13} clearly have larger crystalline domains and smaller average roughness than those grown on SiO_2 surfaces.

The images in Fig. 2d-g and Fig. 4 were taken in "tapping mode" by using FS1500_AuD sensors (Oxford Instruments). The sensitivities for amplitude calibration were determined by a force curve on silicon oxide. The spring constants were determined by the thermal method.[1] The PPP_LFMR sensor gave a spring constant value of 0.85 nN/nm. FS1500_AuD sensors provided spring constants of 3-6 nN/nm, resonance frequencies of 1200-1700 kHz and quality factors of 170-280. For molecular-resolution imaging of PTCDI-C_{13} and dif-TES-ADT in tapping mode, the AFM was operated in the repulsive regime with sub-1 nm set-point amplitudes. Otherwise, amplitudes ranging from 5 to 25 nm were employed. In the latter case, the amplitudes were kept close to the free oscillation amplitude in the attractive regimen to clearly visualize the two organic materials in the phase channel (Fig. S3). Peeling-off scans were performed on the dif-TES-ADT crystal by considerably decreasing the set-point amplitude. The monolayer of dif-TES-ADT on PTCDI-C_{13} was removed by slightly decreasing the set-point amplitude to reach a gently repulsive regimen (Fig. S3).

Structural characterization of semiconductor layer

Out-of-plane XRD measurements were performed in a θ-2θ configuration with a Siemens D5000 X-ray diffractometer. Each measurement took approximately 30 hours and covered a 2θ range of 3° to 23°. With an incidence wavelength of 0.886 Å, the two-dimensional grazing incidence X-ray diffraction (2D-GIXRD) pattern of dif-TES-ADT on PTCDI-C_{13} was obtained at BL14B1 in the Shanghai Synchrotron Radiation Facility. To further confirm the crystallinity and molecular orientation of multilayer dif-TES-ADT/PTCDI-C_{13} films, 2D-GIXRD and out-of-plane XRD were performed on the samples. The GIXRD pattern in Fig. S4a reveals three groups of discrete Bragg diffraction spots rather than a halo, indicating a highly ordered nature. The appearance of the (001) diffraction peak and the series of (01l) and (11l) peaks imply that the crystalline film consists of a layered structure. However, no new diffraction spots appear in the GIXRD pattern, indicating that the in-plane order of the liquid-like dif-TES-ADT layer on PTCDI-C_{13} may be very close to that of the bulk phase above. Out-of-plane XRD was then used to characterize the bulk structure of the dif-TES-ADT films. Sharp diffraction peaks at 2θ = 5.42°, 16.20° and 21.56° can be seen in the graph, which are ascribed to the (001), (003) and (004) planes, respectively. The lattice parameters calculated from both GIXRD and XRD are in good agreement with the HR-AFM and AFM measurements presented in Fig. 1.

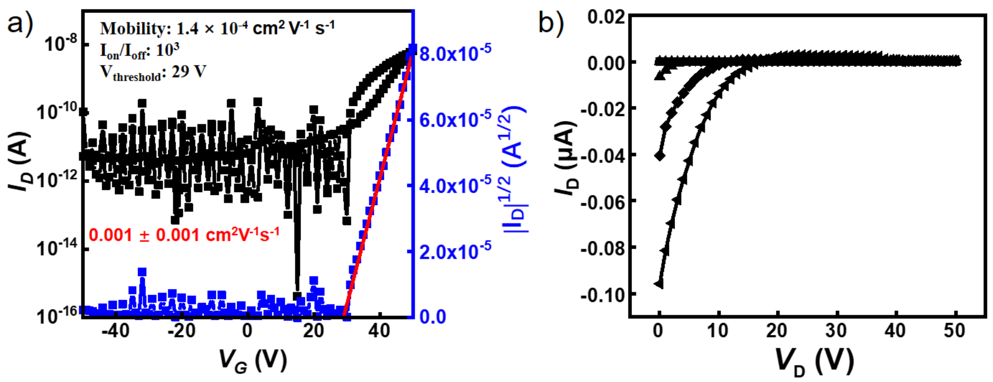

Fig. S1 a-b) The transfer and output curves of a PTCDI-C_{13} monolayer transistor.

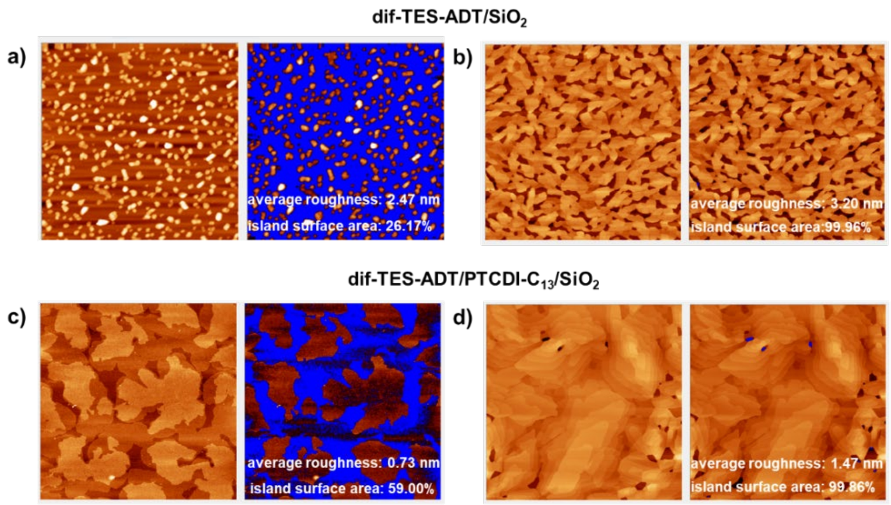

Fig. S2 Actual and corresponding flooded AFM morphology images of **a-b)** dif-TES-ADT/SiO_2 and **c-d)** dif-TES-ADT/PTCDI-C_{13}/SiO_2.

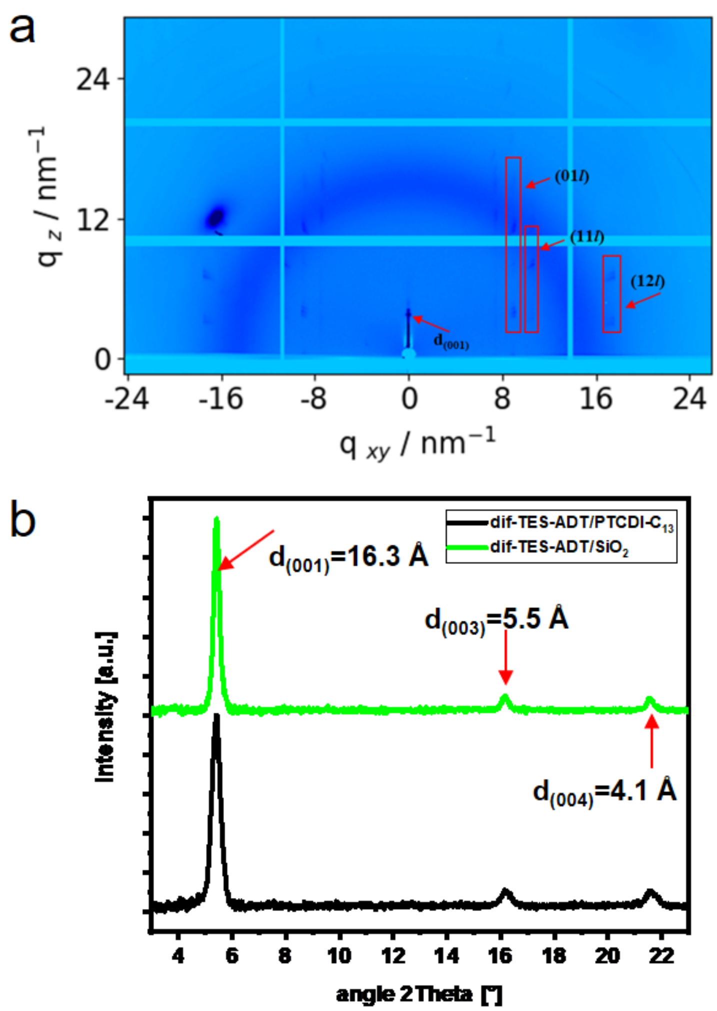

Fig. S3 a) 2D-GIXRD pattern of dif-TES-ADT on PTCDI-C_{13}. **b)** Out-of-plane XRD pattern of multilayer dif-TES-ADT films on different surfaces.

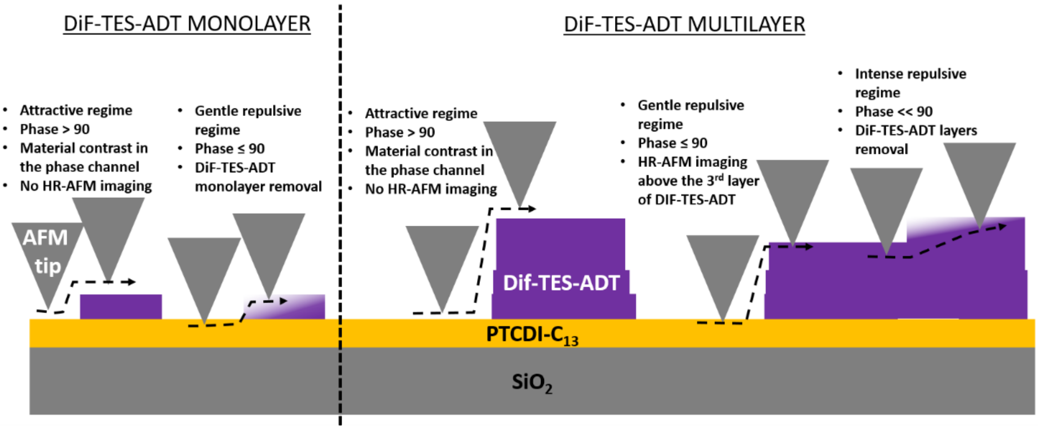

Fig. S4 Scheme of the different force regimes used in tapping mode AFM on dif-TES-ADT monolayer and multilayer samples for either imaging or applying the peeling-off technique.

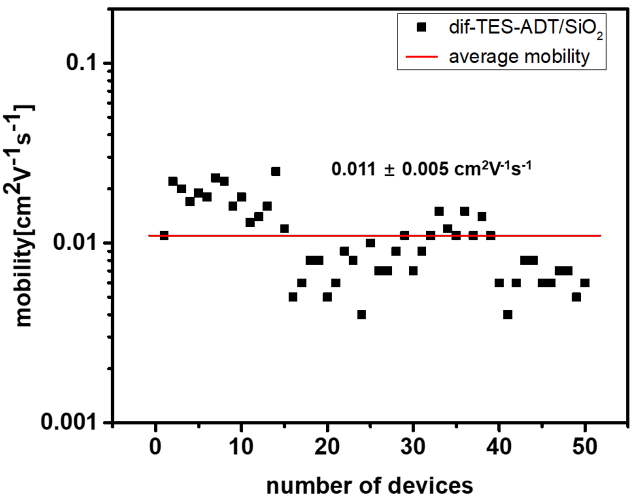

Fig. S5 Distribution of carrier mobilities measured from 50 OFETs based on dif-TES-ADT films on SiO_2.

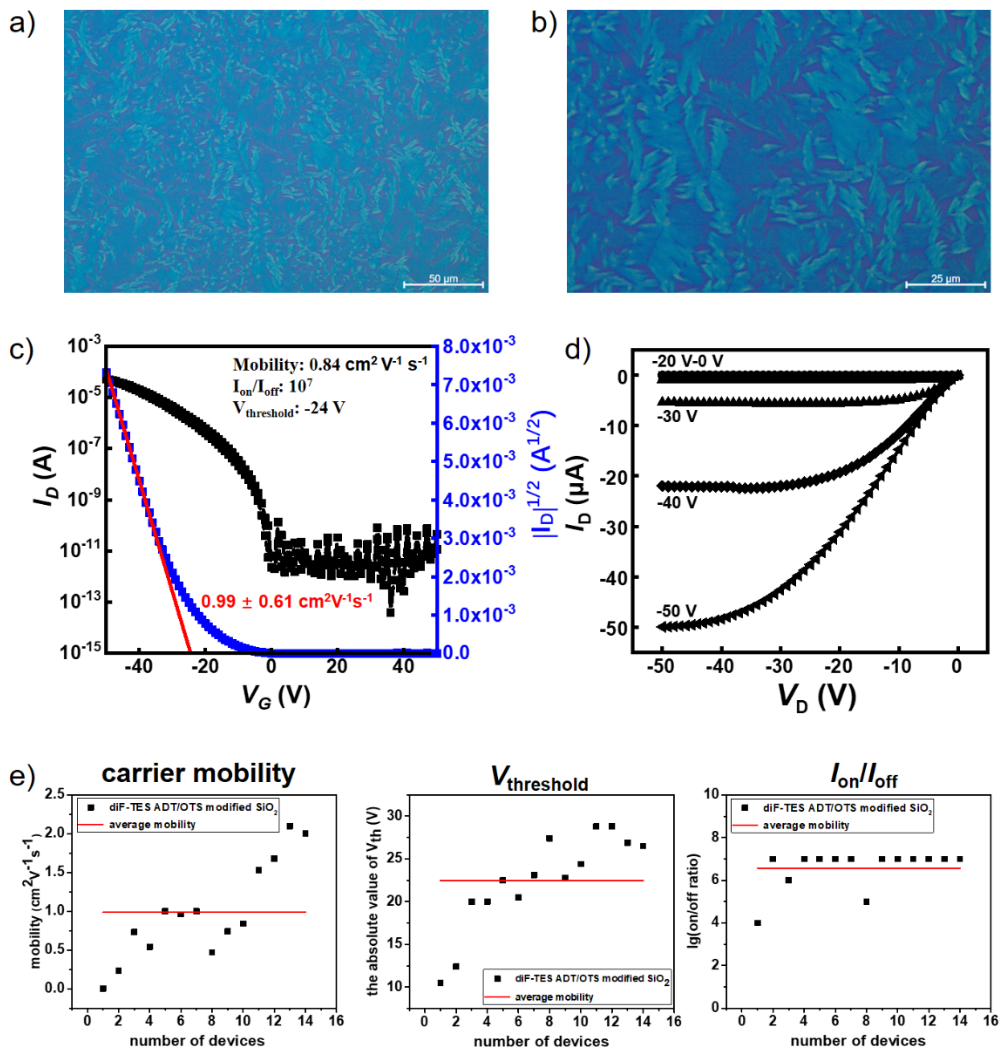

Fig. S6 a-b) Optical microscope images of 15 nm dif-TES-ADT films on OTS-treated SiO_2 surface. **c-d)** The transfer and output curves of a dif-TES-ADT transistor with OTS-treated SiO_2 as the dielectric layer. **e)** Statistics of carrier mobility, threshold voltage and on/off ratio of 14 devices.

References

1. Hutter JL, Bechhoefer J. Calibration of atomic-force microscope tips. Rev Sci Instrum, 1993, 64: 1868–1873